

As a library, NLM provides access to scientific literature. Inclusion in an NLM database does not imply endorsement of, or agreement with, the contents by NLM or the National Institutes of Health.

Learn more: [PMC Disclaimer](#) | [PMC Copyright Notice](#)



FASEB J. 2011 Jan;25(1):428–434. doi: [10.1096/fj.10-170076](https://doi.org/10.1096/fj.10-170076)

Manipulating the permeation of charged compounds through the MscL nanovalve

[Li-Min Yang](#)¹, [Paul Blount](#)^{1,1}

[Author information](#) [Article notes](#) [Copyright and License information](#)

PMCID: PMC3005423 PMID: [20930114](#)

Abstract

MscL is a bacterial mechanosensor that serves as a biological emergency release valve, releasing cytoplasmic solutes to the environment on osmotic downshock. Previous studies have recognized that this channel has properties that make it ideal for use as a triggered nanovalve for vesicular-based targeted drug-release devices. One can even change the modality of the sensor. Briefly, the introduction of charges into the MscL pore lumen gates the channel in the absence of membrane tension; thus, by inserting compounds that acquire a charge on exposure to an alternative stimulus, such as light or pH, into the pore of the channel, controllable nanoswitches that detect these alternative modalities have been engineered. However, a charge in the pore lumen could not only encourage actuation of the nanopore but also have a significant influence on the permeation of large charged compounds, which would thus have important implications for the efficiency of drug-release devices. In this study, we used *in vivo* and electrophysiological approaches to demonstrate that the introduction of a charge into pore lumen of MscL does indeed influence the permeation of charged molecules. These effects were more drastic for larger compounds and, surprisingly, were related to the orientation of the MscL channel in the membrane.—Yang, L-M, Blount, P. Manipulating the permeation of charged compounds through the MscL nanovalve.

Keywords: osmoregulation, drug-release device, ionic preference, ionic selectivity

The mechanosensitive channel of large conductance (MscL) is found in the cytoplasmic membrane of most bacteria (1), where it plays a vital role in osmoregulation by protecting the cell from lysis on acute decreases in external osmotic environment by releasing cytoplasmic osmolytes (2), thus serving as a biological “emergency release valve.” It has remained one of the best studied and most understood of mechanosensitive channels. A MscL homologue from *Mycobacterium tuberculosis* has been resolved by X-ray crystallography and shown to be of simple architecture: a homopentamer, with each subunit containing 2 transmembrane α helices and a cytoplasmic α helical bundle (3). The first transmembrane domain, TM1, forms the pore of the channel, while the second transmembrane domain, TM2, is exposed to the lipid bilayer. In response to tension in cell membrane, both TM1 and TM2 expand, and this expansion ultimately leads to channel opening, with TM1 largely forming the pore lumen (4–7).

Several previous studies have recognized that this channel has many properties that would make it ideal for use in vesicular-based targeted drug-release nanodevices. It has a very large pore size (30–40 Å; ref. 8); thus, when gated, the nanopore would allow large compounds to be released. Furthermore, it can be translated *in vitro* (9) or synthetically synthesized (10), reconstituted into lipids, and yet spontaneously assemble into a functional complex. Moreover, introduction of charges into the MscL pore lumen can gate the channel in the absence of membrane tension (5, 11, 12). This approach has allowed for the engineering of controllable nanopores, or nanoswitches that detect alternative modalities, including light (13) and pH (14). To perform this technique, compounds that acquire charges in response to these stimuli are inserted chemically, by thiol reactions to unique cysteines substituted by site-directed mutagenesis, into the pore of the channel. However, a charge in the pore lumen might not only encourage actuation of the nanopore but also influence the permeation of charged molecules. In this study, we used *in vivo* efflux assays and patch-clamp approaches to address this question.

MATERIALS AND METHODS

Strains and cell growth

The MscL mutants were generated using the Mega Primer method as described previously (15). Mutants were inserted within the pB10b or pB10d expression construct, a modified pB10b plasmid (16–18). *Escherichia coli* strain PB104 ($\Delta mscL:Cm$) (16) was used for *in vivo* assays and electrophysiological analysis. 2-(trimethylammonium)ethyl methanethiosulfonate bromide (MTSET) and 2-sulfonatoethyl methanethiosulfonate sodium salt (MTSES) were obtained from Toronto Research Chemicals Inc. (North York, ON, Canada). Spermine 4HCl and Na₂-succinate were from Sigma-Aldrich (Buchs, Switzerland). Agarose was from Bio-Rad Laboratories, Inc. (Hercules, CA, USA). Unless indicated, cultures were routinely grown in Lennox broth (LB) medium (Fisher Scientific, Fair Lawn, NY, USA) plus

ampicillin (100 µg/ml) in a shaker-incubator at 37°C and rotated at 250 cycles/min. Expression was induced by addition of 1 mM isopropyl-β-D-thiogalactopyranoside (IPTG; Anatrace Inc., Maumee, OH, USA).

In vivo efflux assays

K⁺ efflux assay

E. coli PB104 cells were grown in K10 medium (46 mM Na₂HPO₄, 23 mM NaH₂PO₄, 8 mM (NH₄)₂SO₄, and 10 mM KCl, pH 7) supplemented with 0.4 mM MgSO₄, 3 µM thiamine HCl, 0.2% D-glucose, 6 µM Fe(NH₄)₂(SO₄)₂, and 100 µg/ml ampicillin. When OD_{600nm} reached ~0.2, cells were induced by 1 mM IPTG for 10 min. Three OD_{600nm} units of culture was then transferred to a nitrocellulose filter (MF membrane, 0.45 µm; Millipore; Tullagreen, Carrigtwohill, Ireland) placed on a supporting surface that was connected to a vacuum suction system. After sucking away medium, cells on the filters were treated with 10 mM MTSES⁻ or 1 mM MTSET⁺ in K0 medium (46 mM Na₂HPO₄, 23 mM NaH₂PO₄, 8 mM (NH₄)₂SO₄, and 10 mM NaCl, pH 7) for 15 s. Filters were then washed by 3 ml K0 medium and placed in a 50-ml plastic beaker to dry at 50°C overnight. The solute on the filter was dissolved in 3 ml double-distilled water and assayed for K⁺ by flame photometry (Jenway; Dunmow, Essex, UK).

Glutamate efflux assay

E. coli PB104 cells were grown in K10 medium [46 mM Na₂HPO₄, 8 mM (NH₄)₂SO₄, and 10 mM KCl, adjusted to pH 8.5 with NaOH] with supplements [0.4 mM MgSO₄, 3 µM thiamine HCl, 0.2% D-glucose, 6 µM Fe(NH₄)₂(SO₄)₂, and 100 µg/ml ampicillin] until OD_{600nm} reached ~0.2, then the same amount of prewarmed K10 medium (pH 8.5) with supplements and 1 M NaCl was added to the culture. After 2 h, the cells were induced with 1 mM IPTG for 10 min before being transferred to nitrocellulose filters. Treatment with MTSES⁻ or MTSET⁺ was performed the same way as for the K⁺ assay, except K10 medium plus 0.5M NaCl (pH 7) was used to dissolve the drugs and wash the filters. The filters were then stored at -80°C before measurement of glutamate using a glutamate assay kit (BioAssay Systems, Hayward, CA, USA).

Trehalose efflux assay

E. coli PB104 cells were grown in K10 medium [46 mM Na₂HPO₄, 23 mM NaH₂PO₄, 8 mM (NH₄)₂SO₄, and 10 mM KCl, pH 7] with supplements [0.4 mM MgSO₄, 3 µM thiamine HCl, 0.2% D-glucose, 6 µM Fe(NH₄)₂(SO₄)₂, and 100 µg/ml ampicillin] until OD₆₀₀ reached ~0.2. The culture was then divided into 2 aliquots. The first portion of culture was induced by IPTG for 10 min and was transferred to nitrocellulose filters for drug treatment. The second portion was diluted with the same amount of prewarmed K10 medium (pH 7) with supplements and 1 M NaCl for 2 h before IPTG induction and drug treatment on the filter, which was conducted the same way as for the glutamate measurement. The

filters were stored at -80°C before measurement of trehalose using the phenol-sulfuric acid method ([19](#)). The amount of trehalose was calculated by subtracting values of the first portion culture measurement from that of the corresponding second portion culture measurement, as described previously ([20](#)).

Electrophysiology

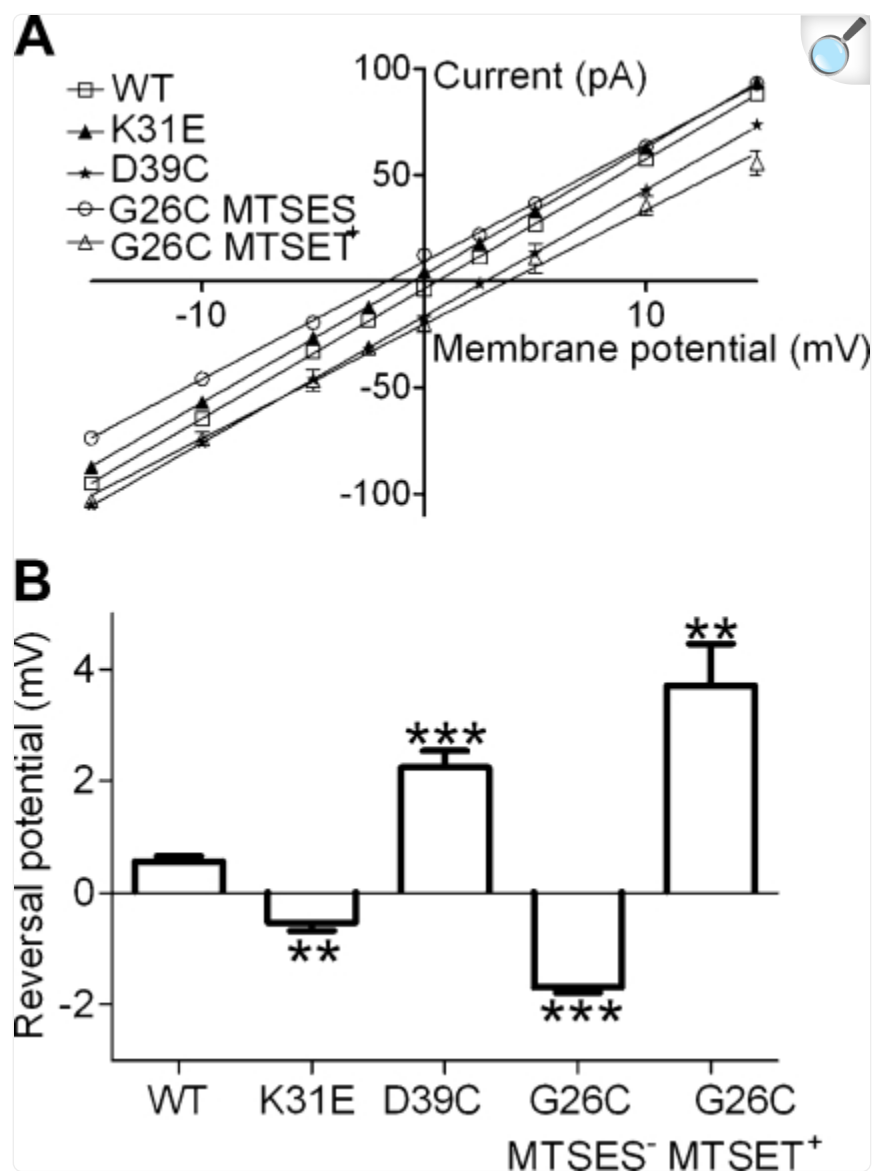
E. coli giant spheroplasts were generated and used in patch-clamp experiments as described previously ([21](#), [22](#)). Excised, inside-out patches were examined at room temperature. Patch buffers used were 200 mM KCl buffer [200 mM KCl, 90 mM MgCl_2 , 10 mM CaCl_2 , and 5 mM HEPES (Sigma, St. Louis, MO), pH 6], 600 mM KCl buffer (600 mM KCl, 90 mM MgCl_2 , 10 mM CaCl_2 , and 5 mM HEPES, pH 6), and low-KCl buffer (10 mM KCl, 40 mM MgCl_2 , and 5 mM HEPES/KOH, pH 6). Spermine 4HCl and Na_2 -succinate were dissolved in low-KCl buffer, and pH was adjusted to 6 with KOH or HCl. Data were acquired at a sampling rate of 20 kHz with a 5-kHz filter, using an AxoPatch 200B amplifier in conjunction with Axoscope software (Axon Instruments, Union City, CA, USA). A piezoelectric pressure transducer (World Precision Instruments, Sarasota, FL, USA) was used to monitor the pressure introduced to patch membrane by suction throughout the experiments. Measurements were performed using Clampfit9 from Pclamp9 (Axon Instruments).

Both MTSES^- and MTSET^+ application by pipette led to spontaneous opening of G26C MscL. MTSES^- (4–10 mM) was applied by pipette to obtain full opening of single channels; sometimes low suction was applied. In most cases, MTSET^+ applied by pipette led to the spontaneous opening of more than one channel, which brought difficulty for single-channel current measurement. We found that MTSET^+ applied in the bath could gate the channel spontaneously after the channel was already opened by pipette suction. This finding is consistent with previous reports about the effect of MTSET^+ on G26C MscL and G22C MscL, a mutation in a similar position of the channel ([5](#), [11](#)). Therefore, 2–4 mM MTSET^+ was applied in bath solution (cytoplasmic side of MscL), and single spontaneous opening of the channel was achieved by opening a single channel by suction to allow access of MTSET^+ . G26C MscL could be opened within a broad range of pressure. In some patches, the pressure required was lower than that for wild-type MscL, while in other patches the pressure applied was much higher than that for wild-type MscL, which is consistent with previous reports ([5](#), [15](#)). This probably is due to different degrees of disulfide bridge formation in excised patches. Measurement of ionic preference was performed as follows: First, the offset was adjusted to 0 under 200 mM KCl buffer symmetric configuration when either MscS or MscL was opened and confirmed by channel reversal potential of 0 mV; Second, the bath solution was changed to 600 mM KCl buffer, and currents were recorded at the voltages shown to allow the current/voltage analysis. The influence of liquid junction potentials was eliminated by using an agarose bridge (2% agarose in 200 mM KCl buffer) as the reference electrode.

RESULTS

It has been assumed that, because of its large pore size, MscL has no ionic preference. Therefore, for this study, we initially sought to determine whether this was indeed the case. We recorded from inside-out patches obtained from giant bacterial spheroplasts, as described previously (21). Using asymmetric conditions, as described in Materials and Methods, the I/V plot of wild-type MscL was generated, and its reversal potential was determined. [Figure 1](#) shows that wild-type MscL has a positive reversal potential of 0.57 ± 0.09 mV. This finding is much closer to the Cl^- reversal potential (17.5 mV) than the reversal potential for K^+ (-27.8 mV), thus indicating an anionic preference.

Figure 1.



[Open in a new tab](#)

Ionic preferences of wild-type and mutant MscL nanopores. *A*) Current-voltage plots of MscL under asymmetric ionic conditions (40 mM MgCl₂, 10 mM CaCl₂, and 5 mM HEPES/KOH, pH 6.0, plus 200 mM KCl in pipette, 600 mM KCl in bath). Reversal potentials for Cl⁻ and K⁺ are +17.5 and -27.8 mV, respectively. Graphs show current-voltage relationships of wild-type (WT) MscL and mutant MscL K31E, D39C, and G26C treated with either MTSES⁻ or MTSET⁺ (*n*=6). *B*) Reversal potentials determined by current-voltage plots in *A*; *n* = 6. ***P* < 0.01, ****P* < 0.001 vs. WT MscL; 2-tailed *t* test.

Several lines of evidence suggest that the first transmembrane domain, TM1, forms the bulk of the lumen of the open-channel pore (4, 5, 7). One possible interpretation of the observed anionic preference of the MscL channel is that of a positive charge in the pore attracting anions and repulsing cations. Because K31 is the only positively charged residue in the TM1 domain of MscL, we studied the effects of mutating this site into a negatively charged residue. As expected, K31E mutant MscL has a reversal potential closer to that of K^+ (-0.53 ± 0.14 mV; Fig. 1A). Hence, although this mutation did not render a cationic preference, it did significantly decrease the anionic preference of the channel.

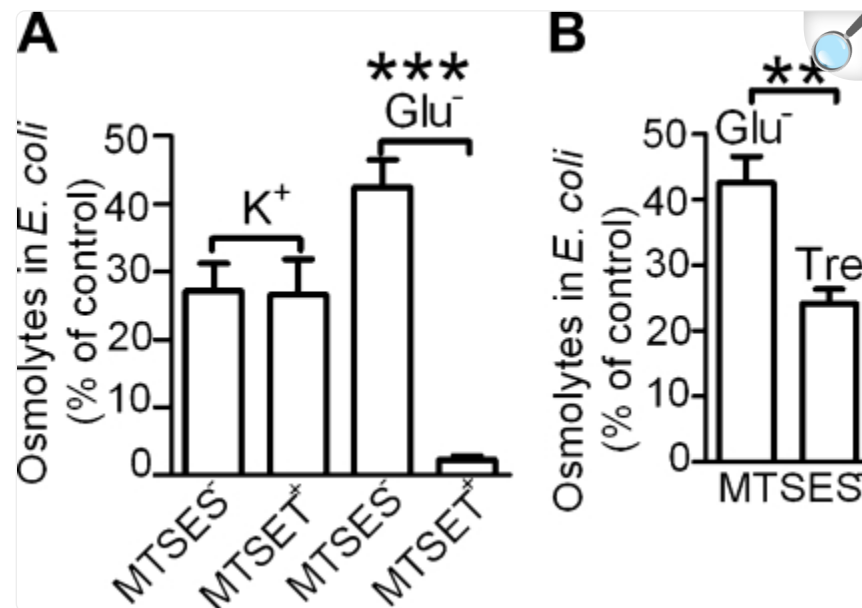
We next addressed the question of whether we could influence ionic preference by manipulating other charges within the TM1 pore domain. There are two negatively charged residues in TM1, D18 and D39. Previously, in a cysteine scan of the region, we demonstrated that a D18C mutation led to a nonfunctional channel (15, 23); D39C, however, is functional (15). We therefore tested the ionic preference of D39C MscL. Consistent with the notion that D39 influences the ionic preference of the channel, we found that this mutant had an increased anionic preference (reversal potential 2.25 ± 0.28 mV; Fig. 1).

Several studies have demonstrated that charges can be engineered within the pore post-translationally by reacting charged sulfhydryl reagents with mutated channels containing unique cysteines, thus leading to a spontaneously gating channel (4, 5, 11). One such MscL mutant, G26C, is especially sensitive to the charged sulfhydryl reagents MTSET⁺ and MTSES⁻ (5). We therefore utilized this approach to investigate potential changes of the ionic preference when the channel is gated by the introduction of a charge within the pore. As shown in Fig. 1, G26C MscL treated with MTSET⁺ had an increased anionic preference compared with that of the wild type MscL (reversal potential of 3.71 ± 0.75 mV), indicating that the introduction of a positive charge into the pore of the MscL nanopore increases the permeation of anions. On the other hand, MTSES⁻ treated G26C MscL had a decreased anionic preference (reversal potential of -1.69 ± 0.09 mV).

Clearly, charges within the pore of MscL not only encourage MscL channel gating (4, 5, 11, 12) but also modulate ionic preferences. Thus, we speculated that such charges would have even greater influences on the permeation of large charged molecules. To maintain turgor, *E. coli* cells accumulate osmolytes, such as K^+ , glutamate⁻, and trehalose, on osmotic upshock (20, 24, 25), and they release these and other osmolytes through MscL to survive osmotic downshock (2, 26–29). With this knowledge, we designed an *in vivo* assay to test the efflux of K^+ , glutamate⁻, and trehalose through G26C MscL modified and thus gated by charged thiol reagents. In the absence of membrane tension, the efflux was achieved when G26C MscL-expressing *E. coli* bacteria were treated with MTSET⁺ or MTSES⁻. As expected, the flux was mutant MscL specific; no efflux was observed from *E. coli* expressing wild-type MscL after MTSET⁺ or MTSES⁻ treatment (data not shown). After MTSET⁺ or MTSES⁻ treatment, <30% of the measurable K^+ remained in cells (Fig. 2A). This value is only slightly higher than that observed from osmotic downshock, where it has been reported that 10–20% of intracellular K^+ is resistant to osmotic-induced flux (30). Therefore, both MTSET⁺ and MTSES⁻ treatments led to the efflux of the vast majority of the available K^+ . Interestingly, the efflux of glutamate⁻, a much larger molecule, showed dramatically more flux after MTSET⁺ treatment than after MTSES⁻ treatment (Fig. 2A). While we suspected

this difference in glutamate efflux was largely due to the charge introduction into channel pore, it could alternatively be because MTSET⁺ more efficiently gates the channel. We therefore determined the flux of glutamate⁻ relative to that of trehalose, which is not charged, on MTSES⁻ treatment. As seen in Fig. 2B, although trehalose is twice the size of glutamate⁻, it is more efficiently fluxed from the cell. Therefore, it appears that the negative charge within G26C MscL, which was introduced by MTSES⁻, decreased the efflux of the negatively charged glutamate⁻ molecule through the channel.

Figure 2.



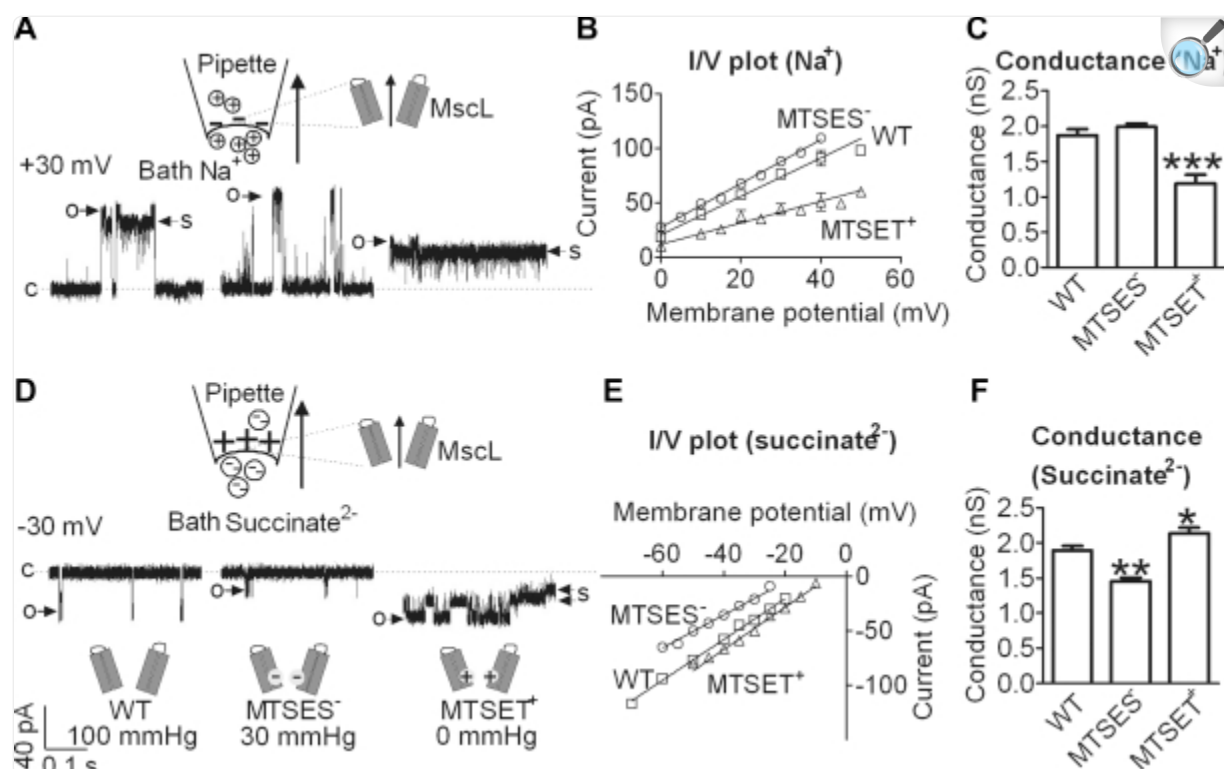
[Open in a new tab](#)

In vivo efflux of osmolytes from *E. coli* expressing G26C MscL. Osmolytes in *E. coli* efflux out of cell after G26C MscL is gated by either MTSES⁻ or MTSET⁺ treatment. Efflux efficiency is expressed as percentage of cell osmolytes before treatment. A) Efflux of K⁺ and glutamate⁻ (Glu⁻). B) Efflux of Glu⁻ and trehalose (Tre); $n = 7$. ** $P < 0.01$, *** $P < 0.001$; 2-tailed t test.

To better determine the molecular basis for permeation of large charged compounds through modified MscL nanovalves, we investigated the permeation of succinate²⁻ and spermine⁴⁺ through the channel in inside-out patches of *E. coli* spheroplast membranes. These two large charged molecules have been reported previously to permeate through wild-type MscL (8). As shown in Fig. 3, when G26C MscL was treated with MTSES⁻, the conductance of succinate²⁻ was decreased significantly when compared with wild-type MscL, again demonstrating that negative charges introduced into the MscL pore inhibit the permeation of larger negatively charged molecules. Interestingly, MTSES⁻-treated G26C

MscL had a significantly increased conductance for spermine⁴⁺ ([Fig. 4](#)). In contrast, when the G26C MscL was treated with MTSET⁺, the conductance for succinate²⁻ was significantly increased ([Fig. 3](#)), and the permeation of spermine⁴⁺, as assessed by conductance, was significantly decreased for the MTSET⁺-treated G26C MscL ([Fig. 4](#)). MTSET⁺-treated G26C MscL displayed a full opening at a membrane potential of 0 mV, which was recorded before the application of each voltage step. At large membrane potentials, it had a propensity for substates (labeled as s in traces of [Figs. 3](#) and [4](#)). Prolonged application of a high membrane potential could lead to sustained substate opening, or even closure of the channel. The all-points histograms of channel openings at different voltage steps are shown in Supplemental Data. Although we cannot completely rule out the possibility that we are measuring a stabilized substate, we did weight the conductance measurements taken at lower membrane potentials where we were more confident in measuring fully open channels. Furthermore, it seems likely that the conductance of the channel measured at low potentials would be representative of the channel permeability as a nanovalve in a liposome reconstitution system. Together, the above data demonstrate that charges within the pore clearly influence the permeation of larger charged molecules: like charges significantly inhibit flux; opposite charges can increase flux.

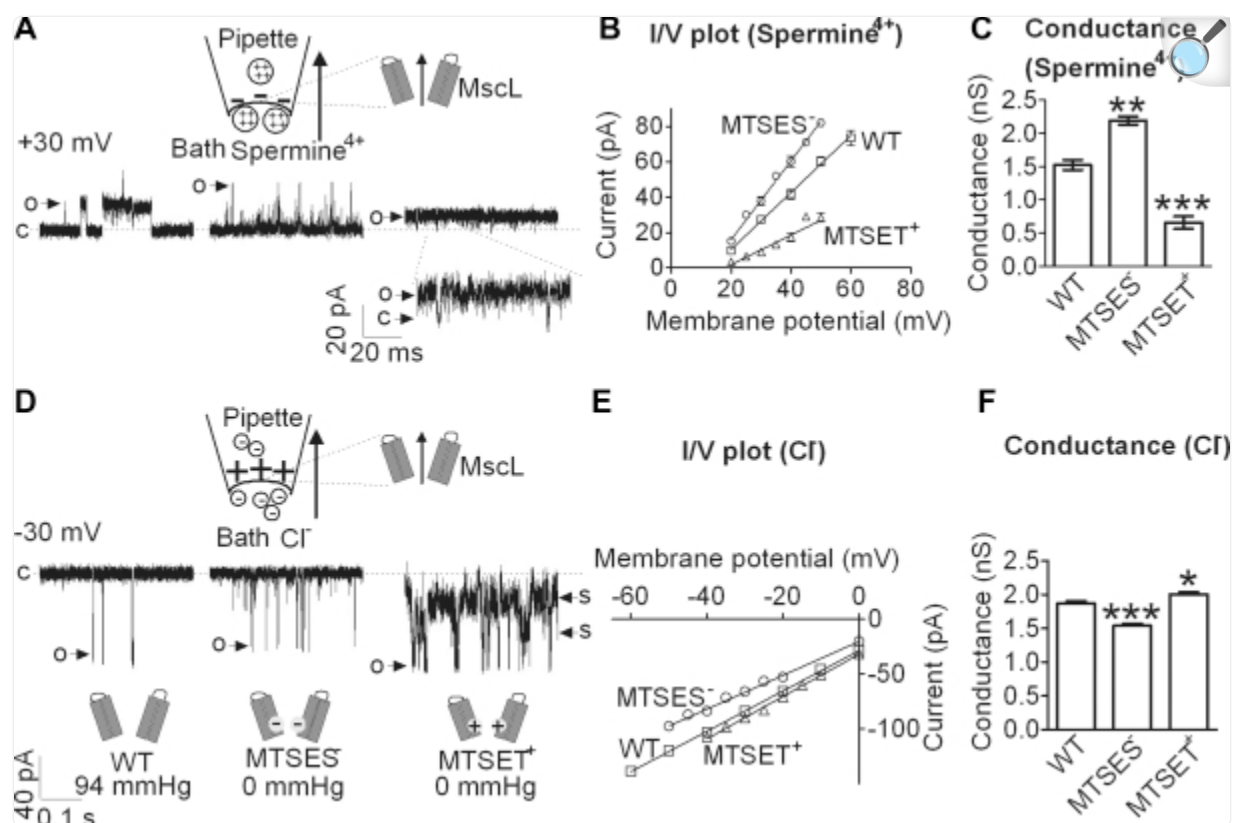
Figure 3.



[Open in a new tab](#)

Permeation of Na₂-succinate through MscL. *A*) Representative current traces of wild-type (WT) MscL (left) and MTSES⁻-modulated (middle) and MTSET⁺-modulated G26C MscL (right) recorded in configuration in which pipette was filled with low-KCl buffer (10 mM KCl, 40 mM MgCl₂, and 5 mM HEPES/KOH, pH 6) and bath solution contained low-KCL buffer supplemented with 300 mM Na₂-succinate with pH adjusted to 6, at which succinate has 2 negative charges, expressed as succinate²⁻. Positive current was mostly due to permeation of Na⁺, because positive membrane potential only allows Na⁺ to pass through MscL from bath. Full single-channel openings and baselines of recordings are indicated as follows: o, open; c, closed; s, substate of channel. Scale bar in *D* applies to all traces. *B*) Current-voltage relationships of single-channel currents for permeation of Na⁺ through wild type (WT) and G26C MscL treated with MTSES⁻ or MTSET⁺. *C*) Conductance of Na⁺ as determined from slopes of current-voltage relationships in *B*. *D–F*) Panels are comparable to *A–C*, respectively; voltage was reversed so that permeation of succinate²⁻ from the bath could be measured. Same pressures were applied for *A* and *D* (indicated in *D*). Pressure needed to open G26C MscL for access of MTSET⁺ was 213 mmHg. *n* = 6. **P* < 0.05, ***P* < 0.01, ****P* < 0.001 vs. WT MscL; 2-tailed *t* test.

Figure 4.





[Open in a new tab](#)

Permeation of spermine 4HCl through MscL. *A*) Representative current traces of wild-type (WT) MscL (left) and MTSES⁻-modulated (middle) and MTSET⁺-modulated G26C MscL (right) recorded in configuration in which pipette was filled with low-KCl buffer (10 mM KCl, 40 mM MgCl₂, and 5 mM HEPES/KOH, pH 6) and bath solution contained low-KCL buffer supplemented with 100 mM spermine 4HCl with pH adjusted to 6, at which spermine has 4 positive charges, expressed as spermine⁴⁺. Positive current is mostly due to permeation of spermine⁴⁺, because positive membrane potential only allows spermine⁴⁺ to pass through MscL from bath. Full single-channel openings and baselines of recordings are indicated as follows: o, open; c, closed; s, substate of channel. Pressures needed to open the channels are shown at bottom. Inset below G26C MTSET⁺ trace shows expansion of indicated section, with scale bar at left. Scale bar in *D* applies to all other traces. *B*) Current-voltage relationships of single-channel currents for permeation of spermine⁴⁺ through wild-type (WT) and G26C MscL treated with MTSES⁻ or MTSET⁺. *C*) Conductance of spermine⁴⁺ as determined by slopes of current-voltage relationships in *B*. *D–F*) Panels are comparable to *A–C*, respectively; voltage was reversed so that permeation of Cl⁻ from bath could be measured. Same pressures were applied for *A* and *D* (indicated in *D*). Pressure needed to open G26C MscL for access of MTSET⁺ was 64 mmHg. *n* = 6. **P* < 0.05, ***P* < 0.01, ****P* < 0.001 vs. WT MscL; 2-tailed *t* test.

For comparison, we also measured the permeation of small ions on pore modifications. As shown in [Fig. 3](#), MTSES⁻ treatment of G26C MscL did not significantly change the conductance of Na⁺. For Cl⁻, we observed a very slight decrease or increase on MTSES⁻ or MTSET⁺ treatment, respectively. These data are consistent with the above findings that permeation of charged molecules is affected by additions of charges within the MscL pore. The result also suggests that the number of charges carried by ions and size of ions matters: larger compounds with more charges are more affected than small ions with fewer charges. This might be due to higher extent of charge repulsion/attraction and lower diffusion coefficient for compounds with multiple charges and large size compared with monocharged ions of small size.

In inside-out patches of *E. coli* spheroplast membranes, the periplasmic side of the channel faces the pipette, while the cytoplasmic side of the channel faces the bath. In the above experiments, the large compounds were added in the bath; therefore, they permeated from the cytoplasmic to the periplasmic side. Since there is bilateral asymmetry of the MscL channel pore in the plane of the membrane, with the pore constriction site located at the cytoplasmic end of the TM1 domain, there may also be asymmetry for the permeation of large charged compounds. Therefore, we tested the flow of spermine⁴⁺ from the periplasmic to the cytoplasmic side of the channel. In this case, spermine 4HCl must be applied by pipette. For unknown reasons, it was difficult to form seals with 100 mM spermine 4HCl in the pipette solution; however, stable seals could be formed when the concentration of spermine 4HCl was reduced to 50 mM. Consistent with the data presented above, and as shown in [Fig. 5](#), when 50 mM spermine⁴⁺ was applied to the bath, its conductance through the MTSES⁻-treated G26C MscL was significantly higher than that through wild-type MscL. Surprisingly, the increase in conductance was not observed when spermine⁴⁺ was applied by the pipette. Similarly, when spermine⁴⁺ was applied to the bath, its conductance through the MTSET⁺-treated G26C MscL pore was decreased significantly compared with that through wild-type MscL; but when spermine⁴⁺ was in the pipette, its conductance was not significantly changed. Together, these data demonstrate not only that the permeation of large charged molecules is influenced by charges in channel pore, but that this influence depends on the orientation of the channel within the membrane.

Figure 5.

MscL	 Peri Cyto		 Peri Cyto	
	Spermine ⁴⁺	Cl ⁻	Spermine ⁴⁺	Cl ⁻
WT	1.49 ±0.03	1.65 ±0.07	1.04 ±0.04	1.44 ±0.06
G26C MTSES ⁻	1.43 ±0.13	1.45 ±0.17	1.67** ±0.03	1.21* ±0.06
G26C MTSET ⁺	1.37 ±0.05	1.68 ±0.07	0.56** ±0.1	1.61** ±0.05

[Open in a new tab](#)

Comparison of spermine 4HCl permeation from periplasmic vs. cytoplasmic side of the MscL channel. Permeation of spermine⁴⁺ and Cl⁻ is expressed as conductance of MscL under negative and positive membrane potential, respectively. Values are means ± SE; *n* = 6. **P* < 0.05, ***P* < 0.01 vs. corresponding wild-type (WT) MscL group; 2-tailed *t* test.

DISCUSSION

In sum, the data demonstrate that, although MscL has a large channel pore (30–40 Å; ref. [8](#)), modifying the charge profile of its pore-forming TM1 domain could either increase or decrease the anionic preference of the channel. Moreover, gating the MscL channel by the insertion of charges can drastically influence the permeation of larger charged compounds, and that this influence depends on the orientation of the channel. These findings have important implications when designing a drug-release device from an engineered MscL nanopore, as previously proposed ([13](#), [14](#), [31](#), [32](#)). To avoid inhibiting the permeation of specific charged drugs or other compounds, one might want to consider the charge used to gate the pore. However, in many instances this might be impractical. For example, low pH is one of the main intrinsic properties that can be found in cancer tissues and inflammation sites in the body, and hence is a common target for triggered drug-delivery devices. However, for such a purpose, a pH-sensitive MscL nanovalve could only be gated by a positive-charge introduction into the channel pore, which could inhibit the release of positively charged drug compounds. Alternatively, it would be advantageous to control the orientation of the nanopore in the

vesicular release device. Normally, the insertion of MscL into liposomal membranes is random (33). However, the direction of a synthetic peptide reconstituted into liposomes has been controlled by inserting a polyethylene glycol (PEG) chain at its end (34). The C terminus of MscL appears to be tolerant to truncation and insertion of tags (16, 17, 35) and thus might be an appropriate location for the addition of such a PEG label, allowing for a cytoplasmic-side-out orientation in a liposome reconstitution system. In this orientation, a charge introduction in the pore would have less influence on the efflux of charged molecules. For both the light sensor and pH sensors previously described (13, 14), the orientation of the sensor might not matter, given that light, and even protons with time, can penetrate the membrane. In addition, it has been reported that a histidine substituted at G22 is accessible to cytoplasmic protons (12). Furthermore, the addition of a PEG group is not likely to be deleterious to the vesicular device; PEG lipids are used routinely in what are termed “stealth vesicles,” because they allow for the evasion of opsonization and uptake by the reticuloendothelial system, and thus have an extended half-life within an organism (36, 37). Overall, nanocarriers are emerging platforms for cancer therapy, and yet the challenge remains in selectively binding and targeting cancer cells (38). Because it has the potential to release therapeutic compounds within or near target tissues on specific stimuli, a controllable MscL nanovalve with high efflux efficiency would be a step toward a selective and efficient nanocarrier.

Supplementary Material

Supplemental Data

[supp_25_1_428_index.html](#) (923B, html)

Acknowledgments

The authors thank Drs. Zoltan Kovacs, Irene Iscla, and Yuezhou Li for many helpful discussions and critical reading of the manuscript.

This work was supported by grant RP100146 from the Cancer Prevention and Research Institute of Texas (CPRIT; <http://www.cprit.state.tx.us>), grant I-1420 of the Welch Foundation, grant NNH08ZTT003N NRA from the U.S. National Aeronautics and Space Administration, and grant GM61028 and its supplement from the U.S. National Institutes of Health.

Footnotes

This article includes supplemental data. Please visit <http://www.fasebj.org> to obtain this information.

REFERENCES

1. Moe P. C., Blount P., Kung C. (1998) Functional and structural conservation in the mechanosensitive channel MscL implicates elements crucial for mechanosensation. *Mol. Microbiol.* 28, 583–592 [[DOI](#)] [[PubMed](#)] [[Google Scholar](#)]
2. Levina N., Totemeyer S., Stokes N. R., Louis P., Jones M. A., Booth I. R. (1999) Protection of *Escherichia coli* cells against extreme turgor by activation of MscS and MscL mechanosensitive channels: identification of genes required for MscS activity. *EMBO J.* 18, 1730–1737 [[DOI](#)] [[PMC free article](#)] [[PubMed](#)] [[Google Scholar](#)]
3. Chang G., Spencer R. H., Lee A. T., Barclay M. T., Rees D. C. (1998) Structure of the MscL homolog from *Mycobacterium tuberculosis*: a gated mechanosensitive ion channel. *Science* 282, 2220–2226 [[DOI](#)] [[PubMed](#)] [[Google Scholar](#)]
4. Bartlett J. L., Levin G., Blount P. (2004) An *in vivo* assay identifies changes in residue accessibility on mechanosensitive channel gating. *Proc. Natl. Acad. Sci. U. S. A.* 101, 10161–10165 [[DOI](#)] [[PMC free article](#)] [[PubMed](#)] [[Google Scholar](#)]
5. Bartlett J. L., Li Y., Blount P. (2006) Mechanosensitive channel gating transitions resolved by functional changes upon pore modification. *Biophys. J.* 91, 3684–3691 [[DOI](#)] [[PMC free article](#)] [[PubMed](#)] [[Google Scholar](#)]
6. Betanzos M., Chiang C. S., Guy H. R., Sukharev S. (2002) A large iris-like expansion of a mechanosensitive channel protein induced by membrane tension. *Nat. Struct. Biol.* 9, 704–710 [[DOI](#)] [[PubMed](#)] [[Google Scholar](#)]
7. Perozo E., Cortes D. M., Sompornpisut P., Kloda A., Martinac B. (2002) Open channel structure of MscL and the gating mechanism of mechanosensitive channels. *Nature* 418, 942–948 [[DOI](#)] [[PubMed](#)] [[Google Scholar](#)]
8. Cruickshank C. C., Minchin R. F., Le Dain A. C., Martinac B. (1997) Estimation of the pore size of the large-conductance mechanosensitive ion channel of *Escherichia coli*. *Biophys. J.* 73, 1925–1931 [[DOI](#)] [[PMC free article](#)] [[PubMed](#)] [[Google Scholar](#)]
9. Berrier C., Park K. H., Abes S., Bibonne A., Betton J. M., Ghazi A. (2004) Cell-free synthesis of a functional ion channel in the absence of a membrane and in the presence of detergent. *Biochemistry* 43,

12585–12591 [[DOI](#)] [[PubMed](#)] [[Google Scholar](#)]

10. Clayton D., Shapovalov G., Maurer J. A., Dougherty D. A., Lester H. A., Kochendoerfer G. G. (2004) Total chemical synthesis and electrophysiological characterization of mechanosensitive channels from *Escherichia coli* and *Mycobacterium tuberculosis*. *Proc. Natl. Acad. Sci. U. S. A.* 101, 4764–4769 [[DOI](#)] [[PMC free article](#)] [[PubMed](#)] [[Google Scholar](#)]

11. Yoshimura K., Batiza A., Kung C. (2001) Chemically charging the pore constriction opens the mechanosensitive channel MscL. *Biophys. J.* 80, 2198–2206 [[DOI](#)] [[PMC free article](#)] [[PubMed](#)] [[Google Scholar](#)]

12. Yoshimura K., Batiza A., Schroeder M., Blount P., Kung C. (1999) Hydrophilicity of a single residue within MscL correlates with increased channel mechanosensitivity. *Biophys. J.* 77, 1960–1972 [[DOI](#)] [[PMC free article](#)] [[PubMed](#)] [[Google Scholar](#)]

13. Koçer A., Walko M., Meijberg W., Feringa B. L. (2005) A light-actuated nanovalve derived from a channel protein. *Science* 309, 755–758 [[DOI](#)] [[PubMed](#)] [[Google Scholar](#)]

14. Koçer A., Walko M., Bulten E., Halza E., Feringa B., Meijberg W. (2006) Rationally designed chemical modulators convert a bacterial channel protein into a pH-sensory valve. *Angew. Chem.* 45, 3126–3130 [[DOI](#)] [[PubMed](#)] [[Google Scholar](#)]

15. Levin G., Blount P. (2004) Cysteine scanning of MscL transmembrane domains reveals residues critical for mechanosensitive channel gating. *Biophys. J.* 86, 2862–2870 [[DOI](#)] [[PMC free article](#)] [[PubMed](#)] [[Google Scholar](#)]

16. Blount P., Sukharev S. I., Moe P. C., Schroeder M. J., Guy H. R., Kung C. (1996) Membrane topology and multimeric structure of a mechanosensitive channel protein of *Escherichia coli*. *EMBO J.* 15, 4798–4805 [[PMC free article](#)] [[PubMed](#)] [[Google Scholar](#)]

17. Blount P., Sukharev S. I., Schroeder M. J., Nagle S. K., Kung C. (1996) Single residue substitutions that change the gating properties of a mechanosensitive channel in *Escherichia coli*. *Proc. Natl. Acad. Sci. U. S. A.* 93, 11652–11657 [[DOI](#)] [[PMC free article](#)] [[PubMed](#)] [[Google Scholar](#)]

18. Moe P. C., Levin G., Blount P. (2000) Correlating a protein structure with function of a bacterial mechanosensitive channel. *J. Biol. Chem.* 275, 31121–31127 [[DOI](#)] [[PubMed](#)] [[Google Scholar](#)]

19. Masuko T., Minami A., Iwasaki N., Majima T., Nishimura S., Lee Y. C. (2005) Carbohydrate analysis by a phenol-sulfuric acid method in microplate format. *Anal Biochem.* 339, 69–72 [[DOI](#)] [[PubMed](#)] [[Google Scholar](#)]

20. Dinnbier U., Limpinsel E., Schmid R., Bakker E. P. (1998) Transient accumulation of potassium glutamate and its replacement by trehalose during adaptation of growing cells of *Escherichia coli* K-12 to elevated sodium chloride concentrations. *Arch. Microbiol.* 150, 348–357 [[DOI](#)] [[PubMed](#)] [[Google Scholar](#)]
21. Blount P., Sukharev S. I., Moe P. C., Martinac B., Kung C. (1999) Mechanosensitive channels of bacteria. *Methods Enzymol.* 294, 458–482 [[DOI](#)] [[PubMed](#)] [[Google Scholar](#)]
22. Martinac B., Buechner M., Delcour A. H., Adler J., Kung C. (1987) Pressure-sensitive ion channel in *Escherichia coli*. *Proc. Natl. Acad. Sci. U. S. A.* 84, 2297–2301 [[DOI](#)] [[PMC free article](#)] [[PubMed](#)] [[Google Scholar](#)]
23. Kumánovics A., Levin G., Blount P. (2002) Family ties of gated pores: evolution of the sensor module. *FASEB J.* 16, 1623–1629 [[DOI](#)] [[PubMed](#)] [[Google Scholar](#)]
24. Epstein W., Schultz S. J. (1965) Cation transport in *Escherichia coli*. *J. Gen. Physiol.* 49, 221–234 [[DOI](#)] [[PMC free article](#)] [[PubMed](#)] [[Google Scholar](#)]
25. Ogahara T., Ohno M., Takayama M., Igarashi K., Kobayashi H. (1995) Accumulation of glutamate by osmotically stressed *Escherichia coli* is dependent on pH. *J. Bacteriol.* 177, 5987–5990 [[DOI](#)] [[PMC free article](#)] [[PubMed](#)] [[Google Scholar](#)]
26. Ajouz B., Berrier C., Garrigues A., Besnard M., Ghazi A. (1998) Release of thioredoxin via the mechanosensitive channel MscL during osmotic downshock of *Escherichia coli* cells. *J. Biol. Chem.* 273, 26670–26674 [[DOI](#)] [[PubMed](#)] [[Google Scholar](#)]
27. Ajouz B., Berrier C., Ghazi A. (1998) Effluxes triggered by osmotic downshock in *E. coli* cells devoid of the mechanosensitive ion channel MscL. *Biophys. J.* 74, 239a [[Google Scholar](#)]
28. Berrier C., Garrigues A., Richarme G., Ghazi A. (2000) Elongation factor Tu and DnaK are transferred from the cytoplasm to the periplasm of *Escherichia coli* during osmotic downshock presumably via the mechanosensitive channel mscL. *J. Bact.* 182, 248–251 [[DOI](#)] [[PMC free article](#)] [[PubMed](#)] [[Google Scholar](#)]
29. Ewis H. E., Lu C. D. (2005) Osmotic shock: a mechanosensitive channel blocker can prevent release of cytoplasmic but not periplasmic proteins. *FEMS Microbiol. Lett.* 253, 295–301 [[DOI](#)] [[PubMed](#)] [[Google Scholar](#)]
30. Nakajima H., Yamato I., Anraku Y. (1979) Quantitative analysis of potassium ion pool in *Escherichia coli* K-12. *J. Biochem.* 85, 303–310 [[DOI](#)] [[PubMed](#)] [[Google Scholar](#)]

31. Kocer A., Walko M., Feringa B. L. (2007) Synthesis and utilization of reversible and irreversible light-activated nanovalves derived from the channel protein MscL. *Nat. Protoc.* 2, 1426–1437 [[DOI](#)] [[PubMed](#)] [[Google Scholar](#)]
32. Kocer-Sagiroglu A., Bulten E., Walko M., Feringa B., Robillard G., Meijberg W. (2005) A sensory valve in liposomal drug delivery systems. *J. Control. Release* 101, 374–376 [[PubMed](#)] [[Google Scholar](#)]
33. Powl A. M., East J. M., Lee A. G. (2008) Anionic phospholipids affect the rate and extent of flux through the mechanosensitive channel of large conductance MscL. *Biochemistry* 47, 4317–4328 [[DOI](#)] [[PMC free article](#)] [[PubMed](#)] [[Google Scholar](#)]
34. Nakatani K., Morita T., Kimura S. (2007) Vertical and directional insertion of helical peptide into lipid bilayer membrane. *Langmuir* 23, 7170–7177 [[DOI](#)] [[PubMed](#)] [[Google Scholar](#)]
35. Blount P., Sukharev S. I., Moe P. C., Nagle S. K., Kung C. (1996) Towards an understanding of the structural and functional properties of MscL, a mechanosensitive channel in bacteria. *Biol. Cell* 87, 1–8 [[PubMed](#)] [[Google Scholar](#)]
36. Gabizon A. A. (2001) Stealth liposomes and tumor targeting: one step further in the quest for the magic bullet. *Clin. Cancer Res.* 7, 223–225 [[PubMed](#)] [[Google Scholar](#)]
37. Immordino M. L., Dosio F., Cattel L. (2006) Stealth liposomes: review of the basic science, rationale, and clinical applications, existing and potential. *Int. J. Nanomedicine*. 1, 297–315 [[PMC free article](#)] [[PubMed](#)] [[Google Scholar](#)]
38. Peer D., Karp J. M., Hong S., Farokhzad O. C., Margalit R., Langer R. (2007) Nanocarriers as an emerging platform for cancer therapy. *Nat. Nanotechnol.* 2, 751–760 [[DOI](#)] [[PubMed](#)] [[Google Scholar](#)]

Associated Data

This section collects any data citations, data availability statements, or supplementary materials included in this article.

Supplementary Materials

Supplemental Data

[supp_25_1_428_index.html](#) (923B, html)

[supp_fj.10-170076_10-170076SuppFig1.pdf](#) (126.3KB, pdf)

[supp_fj.10-170076_10-170076SuppFig2.pdf](#) (134.7KB, pdf)

Articles from The FASEB Journal are provided here courtesy of **The Federation of American Societies
for Experimental Biology**